Lung Cancer 132 (2019) 45–53

Contents lists available at ScienceDirect

Lung Cancer

journal homepage: www.elsevier.com/locate/lungcan

Epidermal growth factor receptor-targeted immunomagnetic liposomes for circulating tumor cell enumeration in non-small cell lung cancer treated with epidermal growth factor receptor-tyrosine kinase inhibitors

Shaohua Cui[a,1], Yiqian Ni[a,1], Yizhuo Zhao[a], Zonghai Li[b], Liwen Xiong[a], Jun Liu[a], Xiaofei Liang[b,**], Liyan Jiang[a,*]

[a] Department of Respiratory Medicine, Shanghai Chest Hospital, Shanghai Jiao Tong University, Shanghai, 200030, PR China
[b] State Key Laboratory of Oncogenes and Related Genes, Shanghai Cancer Institute, Renji Hospital, Shanghai Jiao Tong University School of Medicine, Shanghai, 200032, PR China

ARTICLE INFO

Keywords:
Circulating tumor cells (CTC)
Epidermal growth factor receptor (EGFR)
Liquid biopsy
Non-small cell lung cancer (NSCLC)
Targeted therapy

ABSTRACT

Objectives: To establish a circulating tumor cell (CTC) enrichment system for non-small cell lung cancer (NSCLC) patients who received first-line treatment with epidermal growth factor receptor (EGFR)-tyrosine kinase inhibitors (EGFR-TKI), using EGFR magnetic liposomes (EGFR-ML).

Materials and methods: An inverted evaporation method was used to develop antibody modified EGFR-ML. Peripheral blood was collected from NSCLC patients who underwent first-line EGFR-TKI treatment for CTC enumeration.

Results: Protein electrophoresis, magnetic saturation curve, and ultraviolet absorption spectrum showed successful incorporation of the EGFR antibody on the surface of the magnetic microspheres, and the development of EGFR-ML was ascertained based on cell morphology and particle size. Using EGFR-ML, CTC were successfully enriched from blood samples and were identified in 77.3% (99/128) of the cohort. When compared to the 21L858R variant, EGFR-19del showed lower CTC counts by EGFR-ML (CTC_{EGFR}). At one month after EGFR-TKI, a lower CTC_{EGFR} was associated with partial response (PR) during treatment (CTC_{EGFR} < 6 vs. ≥ 6/7.5 mL, 75% vs. 49%, $P = 0.027$). In addition, patients with a lower CTC_{EGFR} at 3 months after EGFR-TKI achieved a longer progression-free survival (PFS) [CTC_{EGFR} < 6 vs. ≥ 6/7.5 mL, 13 months vs. 10.4 months, HR = 2.4, $P = 0.042$]. CTC_{EGFR} significantly increased at the time of RECIST-progressive disease (RECIST-PD). Representative cases showed that CTC_{EGFR} might increase before and beyond RECIST-PD until no clinical benefit could be acquired from EGFR-TKI.

Conclusion: We showed that establishing a CTC enrichment system by antibody modified EGFR-ML in NSCLC is feasible. CTC enumeration by EGFR-ML may have the potential to supplement RECIST in dynamically monitoring the response of NSCLC patients' to first-line EGFR-TKI.

Abbreviations: AFM, atomic force microscope; ARMS, amplification refractory mutation system; CTC, circulating tumor cells; EGFR, epidermal growth factor receptor; EMT, epithelial-mesenchymal transition; EpCAM, epithelial cell adhesion molecule; FA, folic acid; IASLC, The International Association For The Study of Lung Cancer; ML, magnetic liposomes; NCCN, National Comprehensive Cancer Network; NSCLC, non-small cell lung cancer; PAGE, polyacrylamide gel electrophoresis; PBS, phosphate buffer solution; PD, progressive disease; PR, particle response; RECIST, Response Evaluation Criteria in Solid Tumors; SD, stable disease; TKI, tyrosine kinase inhibitors

* Corresponding author at: Department of Respiratory Medicine, Shanghai Chest Hospital, Shanghai Jiao Tong University, No.241 West Huaihai Road, Shanghai, 200030, PR China.

** Corresponding author at: State Key Laboratory of Oncogenes and Related Genes, Shanghai Cancer Institute, Renji Hospital, Shanghai Jiao Tong University School of Medicine, No.25/Ln2200 Xie Tu Road, Shanghai, 200032, PR China.

E-mail addresses: xfliang@shsci.org (X. Liang), Jiang_liyan2000@126.com (L. Jiang).

[1] Shaohua Cui and Yiqian Ni contributed equally to this article.

https://doi.org/10.1016/j.lungcan.2019.04.003
Received 14 February 2019; Received in revised form 2 April 2019; Accepted 4 April 2019

1. Introduction

Driver gene identification and targeted drug discovery have been critical milestones in the diagnosis and treatment of patients with advanced non-small cell lung cancer (NSCLC). Epidermal growth factor receptor (EGFR), which is mutated in ~20% of Caucasian and ~50% of East Asian NSCLC patients [1,2], was the first driver gene identified in NSCLC patients [3,4]. The National Comprehensive Cancer Network (NCCN) Clinical Practice Guidelines for NSCLC recommends EGFR-tyrosine kinase inhibitors (EGFR-TKI) as first-line therapies for advanced NSCLC patients harboring EGFR sensitive mutations [5]. Dynamic monitoring of EGFR mutations during EGFR-TKI treatment is critical for predicting drug resistance [6]. However, due to invasive nature, serial biopsies are impractical in clinical practice [7,8].

Circulating tumor cells (CTC) are tumor cells that have detached from the primary tumor, and shed into the circulation. CTC may localize to distant organs, and therefore aid in metastasis [9,10]. Importantly, the genomic profiles of CTC can reflect the molecular landscape of the overall tumor cell population at the peripheral blood level [11,12], thereby indicating their potential as a "liquid biopsy" biomarker for continuous clinical monitoring of mutations. In previous studies, it has been indicated that the CTC count can be a prognostic and predictive biomarker for cancer patients [13–16]. The isolation and detection of CTC is based on certain distinct physical and biological properties of CTC compared to normal cells. Prospective studies have led to the approval of the CellSearch Platform as a prognostic assay in various cancer types, including breast, prostate and colorectal cancer [17–19]. In the context of NSCLC, baseline CTC counts by CellSearch Platform were associated with the radiographic response to treatment with erlotinib and pertuzumab [16].

However, the CellSearch system relies on the expression of the epithelial cell adhesion molecule (EpCAM) for capturing CTC, and thereby overlooks the CTC with downregulated EpCAM expression due to epithelial-mesenchymal transition (EMT). Therefore, CellSearch may not be an appropriate method for CTC enrichment in highly metastatic cancers, including NSCLC. We have previously established robust techniques for developing monodispersed and functional magnetic polymeric liposomes [20,21]. In this study, we first developed a CTC enrichment system based on EGFR magnetic liposomes (EGFR-ML). Subsequently, we studied the correlation between CTC counts and EGFR-TKI efficacy over the course of treatment by EGFR-ML, in comparison to EpCAM magnetic liposomes (EpCAM-ML) and folic acid magnetic liposomes (FA-ML).

2. Materials and methods

2.1. Study design

Firstly, we constructed a functional EGFR-ML with EGFR antibodies, as outlined in Fig. 1A. Briefly, after preparing the antibody-glycidyl hexa didecyldimethylammonium chloride (GHDC) precursors, an inverted evaporation method embedding Fe_3O_4 magnetic nano-particles into the double-layer membrane structure of liposomes was adopted to establish an antibody modified magnetic liposome system. Subsequently, the CTC-capturing ability of EGFR-ML in phosphate buffer solution (PBS) and simulated whole blood was evaluated *in vitro*, by calculating the recovery rate of CTC modeled by NSCLC cell lines. Peripheral blood samples were collected from NSCLC patients to determine levels of CTC at baseline, 1 month and/or 3 months after EGFR-TKI treatment, as well as at the time of progressive disease (PD). CTC were enriched by the EGFR-ML, EpCAM-ML, and FA-ML, and were enumerated for comparison. Furthermore, patients were also imaged to evaluate the response to EGFR-TKI after one month and subsequently every two months after EGFR-TKI administration (Fig. 1B). Hereafter, CTC_{EGFR}, CTC_{EpCAM}, CTC_{FA}, and CTC_{Total} were used to represent CTC counts by three different ML (EGFR-ML, EpCAM-ML, and FA-ML), and the total CTC numbers, respectively.

2.2. Cell lines and reagents

NSCLC cell lines A549 and LTEP-a-2 were obtained from the American Type Culture Collection (ATCC, Manassas, VA, USA). Dulbecco's Modified Eagle's Medium (DMEM), fetal calf serum (FCS), and trypsin were purchased from Gibco. Antibodies directed against EpCAM (catalog # ab71916), EGFR (catalog # ab52894), cytokeratin (CK) 8, 18, and 19-FITC (catalog # ab41825) were purchased from Abcam, and anti-CD45-PE (catalog # MHCD4504) was from eBioscience. DAPI staining solution (catalog # C1002), FA (catalog # F7876), and DSAPC-APCG (,catalog # 880133) were purchased from Beyotime Biotechnology, Sigma-Aldrich, and Avanti, respectively. EpCAM antibody derivative (catalog # JKAD0001) and magnetic nanoparticles (catalog # JKMN0001) were purchased from Jukang Biotechnology (Shanghai, China). An OLYMPUS B × 61 fluorescence microscope was used to observe CTC.

2.3. Construction of EGFR-ML

EGFR-targeted magnetic immune liposomes were prepared using the thin layer evaporation method for which the detailed process and use of reagents were described previously [21,22]. Briefly, DOPC, phosphatidyl ethanolamine-polyethylene glycol 2000, cholesterol, hexadecyl quaternised chitosan, and magnetic nanoparticles were dissolved in chloroform. After incubation, the mixture was vaporized using a rotary evaporator to form a thin film at the bottom of the flask. Then, 0.1 mol/L PBS (pH = 7.0) was added to dissolve the thin film, mixed, and then placed on a magnetic separation rack to separate the ML. The washing and separation steps were repeated for totally three times. Coupling agents 1-(3-dimethyaminopropyl)-3-ethylcarbodimide hydrochloride [1-ethyl-3-(3-dimethylaminopropyl)carbodiimide, EDC], and N-hydroxy succinimide (NHS), and EGFR antibody (7 μL) were added, and the mixture was incubated for 24 h. After magnetic separation, EGFR-modified ML were obtained and were named EGFR-ML.

2.4. Identification of EGFR-ML characteristics

To validate the EGFR antibodies incorporated on the surface of EGFR-ML, polyacrylamide gel electrophoresis (PAGE) was performed. Atomic force microscope (AFM) was used for the microstructural observation of the ML, and Zetasizer Nano-ZS 90 (Malvern Instruments Ltd., UK) was used to determine particle size and electric potential of the ML. PPMS-9 (QUANTUM DESIGN, USA) was used to detect the hysteresis loop of magnetic particles. Next, an ultraviolet (UV) spectrophotometer was used to scan the UV absorption peak of the EGFR-ML solution to further confirm the presence of the surface antibodies, which were quantified using a BCA protein assay kit.

2.5. Patient selection criteria

In this study, 128 NSCLC patients with EGFR-activating mutations who were admitted to the Department of Respiratory Medicine, Shanghai Chest Hospital, Shanghai Jiao Tong University between December 2015 and August 2017 were included. All patients were histologically diagnosed with advanced NSCLC (stage IIIB/IV according to the tumor-nodule-metastasis system of The International Association For The Study of Lung Cancer, (IASLC)). All patients' tumor samples were confirmed to harbor EGFR-activating mutations identified by the amplification refractory mutation system (ARMS) method. All patients received first-line EGFR-TKI treatment. All patients had baseline CTC enumeration, and CTC counts at one month and/or three months after EGFR-TKI treatment. Patients who lacked clinical information at baseline, response evaluation data of the first 6 months of EGFR-TKI treatment (except for those occurred PD), and had chemotherapy as a

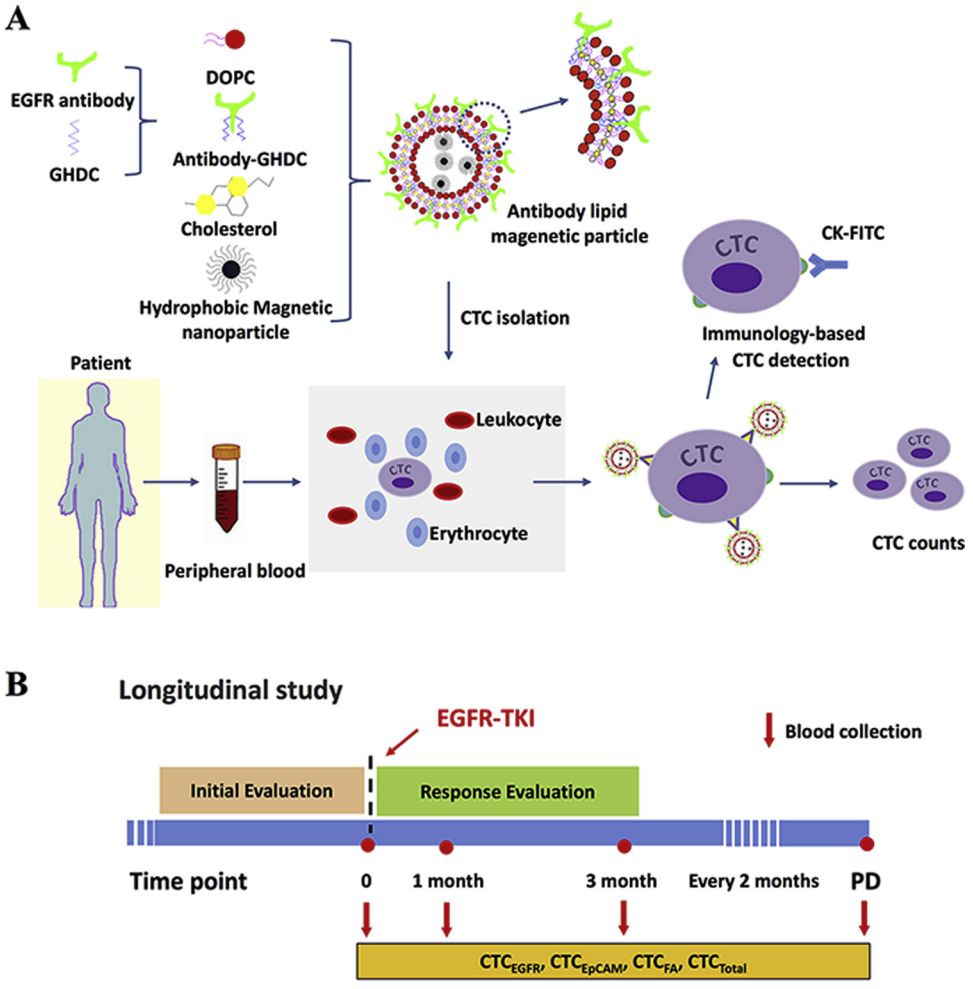

Fig. 1. Schematic overview of study design.
(A) Schematics of EGFR-ML preparation and CTC detection.
(B) Time line of clinical sample collection and patient follow-up. CTC counts using three different ML were measured at baseline, and at 1 month and/or 3 months after EGFR-TKI treatment, and at the time of PD.
CTC, circulating tumor cells; EGFR-TKI, epidermal growth factor receptor tyrosine kinase inhibitors; GHDC, glycidyl hexa didecyldimethylammonium chloride; ML, magnetic liposomes; PD, progressive disease.
CTC_{EGFR}, CTC_{EpCAM}, CTC_{FA}, CTC_{Total} are used to represent CTC counts by different ML and total CTC numbers, respectively.

simultaneous treatment were excluded from the study.

This study was approved by the Ethics Committee of Shanghai Chest Hospital, Shanghai Jiao Tong University (Ethical approval number: KS15-21). All eligible patients provided written informed consent before baseline evaluation.

2.6. CTC capture and identification

Established EGFR-ML were used to sort CTC in PBS or blood samples. For *in vitro* capture evaluation, a single cell suspension of A549 and LTEP-a-2 cells was prepared in 7.5 mL PBS or blood (200 cells per sample). For CTC capture using patient blood samples, a total of 7.5 mL peripheral blood was taken from each patient at each follow-up time point into ethylene diamine tetra-acetic acid (EDTA)-coated tubes. Each anti-coagulated blood sample was divided into three 2.5 mL aliquots, and centrifuged at 1500 rpm for 10 min at room temperature. The middle- and upper-layers were carefully aspirated and mixed with isopycnic PBS (pH = 7.5). Thereafter, 30 μL of EGFR-ML, EpCAM-ML, and FA-ML each were, respectively, added per aliquot of each sample, and incubated for 30 min at room temperature with regular mixing every 5 min. The tubes were then inserted into a magnetic separation rack, and placed for 15 min to remove the supernatant. Captured cells were washed with 1 mL PBS, and incubated with DAPI (30 μL), CK8,18,19-FITC (20 μL) and CD45-PE (20 μL) in the dark for 15 min. Magnetic nanoparticles were removed by a 10 min with PBS, and another 10 min wash with double distilled water. Finally, 30 μL deionized water was added, splattered on slides and air dried, and observed under a fluorescence microscope. Cells with diameters between 8–30 μm, and with strong blue and green fluorescence signals were identified as CTC.

2.7. EGFR-TKI administration and follow-up

All patients received one of the three first-generation EGFR-TKI in one-month cycles. Gefitinib or erlotinib was administered, respectively, at 250 mg and 150 mg once daily, and icotinib at 125 mg three times daily. Prior to initiation of therapy, the baseline of all patients was evaluated. Tumor response to EGFR-TKI was assessed after the first cycle and subsequently after every 2 treatment cycles according to the Response Evaluation Criteria in Solid Tumors (RECIST) version 1.1. To assess the response to EGFR-TKIs, chest CT scans, abdominal ultrasound and standard laboratory tests were routinely performed during EGFR-TKI treatment. Enhanced MRI of the brain and bone scans were performed when necessary. The cut-off date for this study was January 10th, 2018.

2.8. Statistical analysis

Four analyses were conducted using all CTC counts (CTC_{EGFR}, CTC_{EpCAM}, CTC_{FA}, and CTC_{Total}) and clinical characteristics: (1) the correlation between clinical parameters and baseline CTC counts (128 patients), (2) correlation between EGFR-TKI efficacy (including one month response and best response according to RECIST) and CTC counts (84 patients), (3) correlation between PFS and CTC (55 patients), and (4) CTC trend analysis for patients with PD (22 patients). Finally, 3 representative patients were chosen for case presentation. All cohorts are delineated in Figure S1. Based on the median CTC counts detected by each ML, the patients were divided into the CTC low (< 6/7.5 mL peripheral blood) and high (≥ 6/7.5 mL) groups. The cutoff for the CTC low/high groups based on total CTC counts was 5 per 7.5 mL

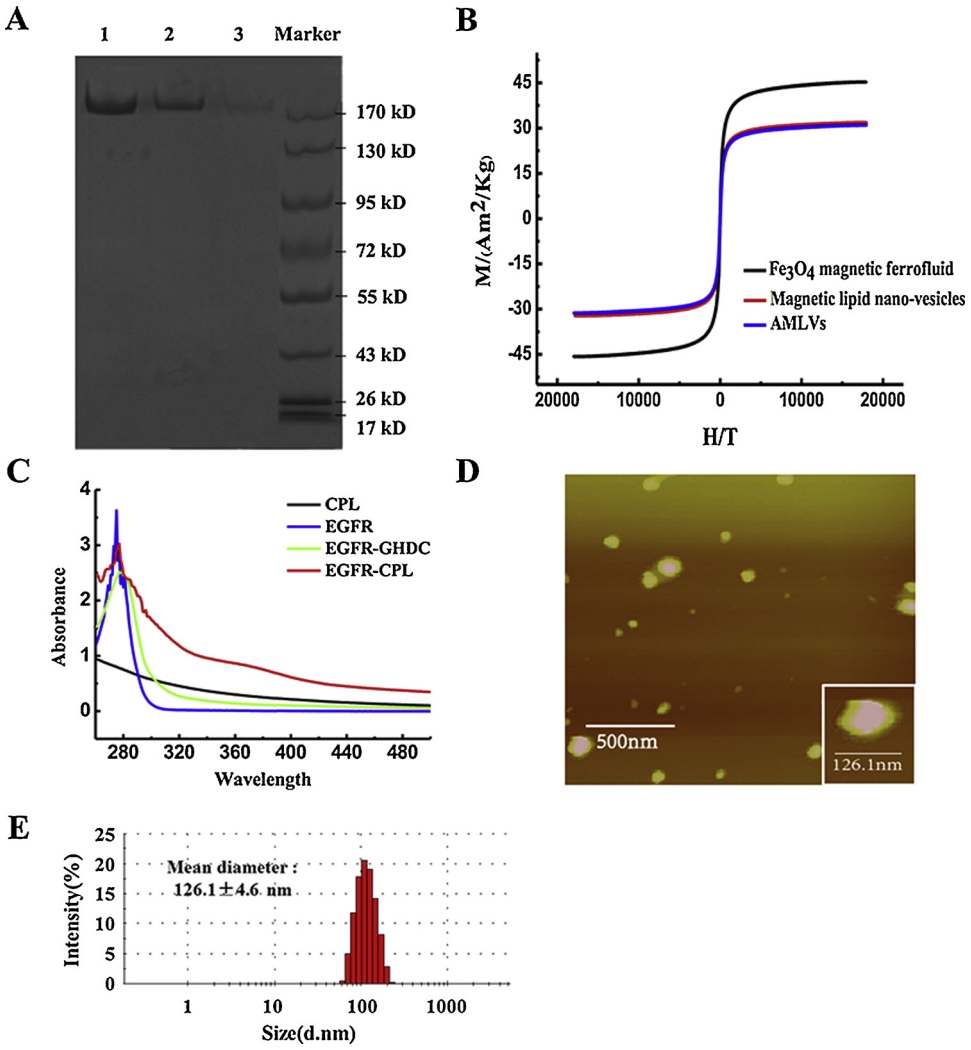

Fig. 2. Material characterizations of functional EGFR-ML.
(A) PAGE analysis of the anti-EGFR antibody and its derivatives. EGFR antibody (lane #1), EGFR-GHDC (lane #2), and EGFR-ML (lane #3);
(B) Magnetic saturation curves of the Fe_3O_4 ferrofluid, magnetic lipid nano-vesicles, and EGFR-ML.
(C) Ultraviolet absorption spectrum of the EGFR antibody, EGFR-GHDC, and EGFR-ML.
(D) Morphology of EGFR-ML by atomic force microscopy.
(E) Size distribution of EGFR-ML magnetic particles based on nanosize and nanosight.
EGFR-ML, epidermal growth factor receptor magnetic liposomes; PAGE, polyacrylamide gel electrophoresis.

blood. Both groups were compared regarding treatment efficacy and PFS at baseline, 1 month or 3 months after treatment, as well as CTC change during treatment. The latter was defined as the change in CTC numbers after treatment (1 month, or 3 months data if the former was unavailable), and patients were divided into the "decreased/unchanged" and "increased" groups accordingly. For the 22 cases with PD, the change in CTC numbers between the 3 months (or 1 month if the former was unavailable) treatment milestone and onset of PD was calculated.

Pearson χ^2 and Fisher's exact tests were used for comparison of the clinical characteristics and treatment responses between the CTC low and high groups. Changes in CTC number between two different time points were compared using non-parametric tests. PFS was defined as the time from the date EGFR-TKI were first administered to the date of objective PD according to RECIST, or until the death of the patient. Kaplan-Meier survival analysis and log-rank tests were used to compare PFS between two groups. Cox regression analysis was employed for multivariate survival analysis, and the hazard ratio (HR) calculation. All confidence intervals reported were 2-sided, and P values < 0.05 were considered statistically significant. Statistical analyses were performed using IBM SPSS® version 22 software (IBM, Armonk, NY, USA).

3. Results

3.1. Characterization of functional EGFR-ML

The presence of EGFR antibodies on EGFR-ML and EGFR-GHDC were confirmed by PAGE (Fig. 2A), and the magnetic saturation curve showed that EGFR-ML had a high magnetic saturation (Fig. 2B). Neither Fe_3O_4-HMN nor EGFR-ML curves showed magnetic hysteresis but instead showed closed hysteresis. In addition, within the permissible range of instrument precision, the remanence and coercive force of both were nearly zero, demonstrating considerable superparamagnetism. The maximum saturation magnetization of Fe_3O_4 magneto fluid and EGFR-ML were 27.9 emu/g and 61.3 emu/g, respectively, indicating 46% purity of the magneto fluid. The UV absorption spectrum of the anti-EGFR antibodies, EGFR-GHDC, and EGFR-ML each showed an absorption peak at 280 nm (Fig. 2C). However, due to denaturation of the antibodies and the impact of nanospheres on UV absorption, the

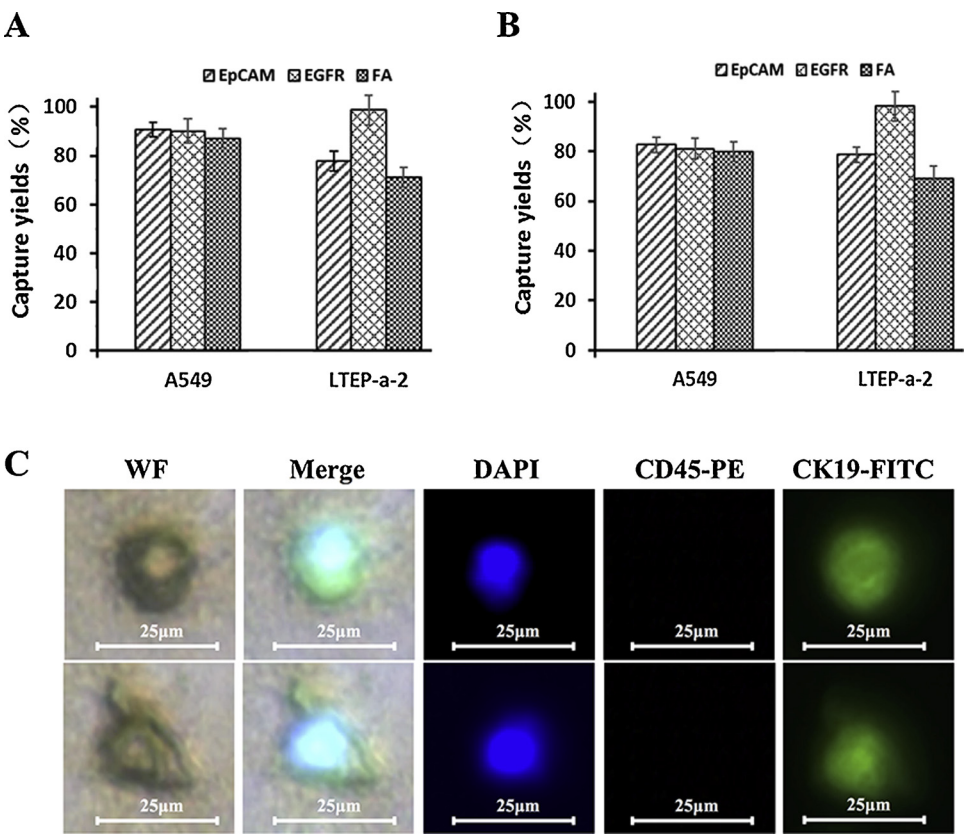

Fig. 3. CTC enrichment by MLs in PBS and peripheral blood samples.
(A) Efficiency of EGFR-ML, EpCAM-ML and FA-ML in capturing A549 and LTEP-a-2 cells in PBS.
(B) Efficiency of EGFR-ML, EpCAM-ML and FA-ML in capturing A549 and LTEP-a-2 cells in simulated whole blood.
(C) Immunofluorescence observation of CTC in clinical blood samples captured by EGFR-ML at 400X magnification.
CTC, circulating tumor cells; EGFR, epidermal growth factor receptor; EpCAM, epithelial cell adhesion molecule; FA, folic acid; ML, magnetic liposomes; PBS, phosphate buffer solution.

absorption peaks of the antibody derivatives and the ML were weaker and wider, which further confirmed successful incorporation of the antibodies on the magnetic microspheres. The antibody level on magnetic microspheres was quantified using the BCA method and was found to be 0.1 mg/mg per microsphere. Microscopic examination showed that the immuno-magnetic microspheres had irregular spherical structures with a maximum diameter of 200 nm and the vesicular features of liposomes with a differential distribution (Fig. 2D). The particle size analyzer indicated an average particle size of 185.2 nm of the nano-ML, which increased to 200.8 nm following EGFR-antibody incorporation (Fig. 2E).

3.2. CTC enrichment by EGFR-ML

EGFR-ML, EpCAM-ML, and FA-ML were able to capture 90.1%, 90.8%, and 87.2%, respectively, of A549 cells from PBS. The recovery rates of LTEP-a-2 cells were 98.7%, 77.9%, and 71.2% by EGFR-ML, EpCAM-ML, and FA-ML, respectively (Fig. 3A). In the simulated whole blood model, the recovery rates of A549 cells were 81.1%, 82.6%, and 79.9%. The recovery rates of and LTEP-a-2 cells were 98.1%, 78.6%, and 69.1% by EGFR-ML, EpCAM-ML, and FA-ML, respectively (Fig. 3B). CTC were also successfully enriched from blood samples derived from EGFR-positive NSCLC patients. Representative images of CTC stained with fluorescent antibodies are shown in Fig. 3C. Under white field, both cell-bound and free EGFR-ML were observed. In addition, the captured CTCs were strongly positive for CK8, CK18, and CK19, but negative for CD45.

3.3. Clinical characteristics and CTC counts

The characteristics of the 128 patients included in this study are shown in Table S1. The correlation between CTC counts and clinical parameters is shown in Table S2. CTC were identified in 99 (77.3%), 93 (72.7%) and 93 (72.7%) of the 128 patients, respectively, by EGFR-ML, EpCAM-ML and FA-ML. Patients with the EGFR-19del mutation were more likely to have a lower CTC_{EGFR} than patients with the 21L858R mutation. The CTC_{EGFR} low group included 58% of the 19del and 40% of the 21L858R group ($P = 0.049$; Fig. 4A). However, no significant correlation was observed between EGFR mutations and CTC_{EpCAM}, CTC_{FA} and CTC_{Total} (Table S2, Fig. 4A).

3.4. EGFR-TKI response and CTC counts

The characteristics of 84 patients are shown in Table S3. Twenty-nine (34%) of 84 patients achieved PR while 55 (66%) of 84 patients achieved SD one month after EGFR-TKI treatment. During the course of EGFR-TKI treatment, 51 patients (61%) achieved PR and 33 patients (39%) achieved SD, resulting in an overall response rate of 61% and disease control rate of 100%. Information regarding baseline CTC counts, and that after 1 month and 3 months of EGFR-TKI treatment are shown in Table S4. No significant changes were observed between 1 month vs. baseline, 3 months vs. baseline, or 3 months vs. 1 month CTC by all the ML (data not shown).

The correlation between CTC counts and the response to first-line EGFR-TKI is shown in Table S5. CTC_{EGFR} at 1 month correlated with patients' best response (low vs. high, 75% PR vs. 49% PR, $P = 0.027$; Fig. 4B, upper panel). Patients with decreased/unchanged CTC_{EGFR} were more likely to achieve PR after 1 month compared to those with increased CTC_{EGFR} (42% vs. 22%, $P = 0.056$; Fig. 4B, middle panel). In addition, patients with a decreased/unchanged CTC_{EGFR} (67% vs. 50%, $P = 0.115$; Fig. 4B, middle panel) or CTC_{Total} (44% vs. 26%, $P = 0.078$; Fig. 4B, lower panel) at 1 month or 3 months were more likely to achieve PR during EGFR-TKI treatment when compared to patients with increased CTC_{EGFR}. However, no correlation was observed between EGFR-TKI response and CTC_{EpCAM} and CTC_{FA}.

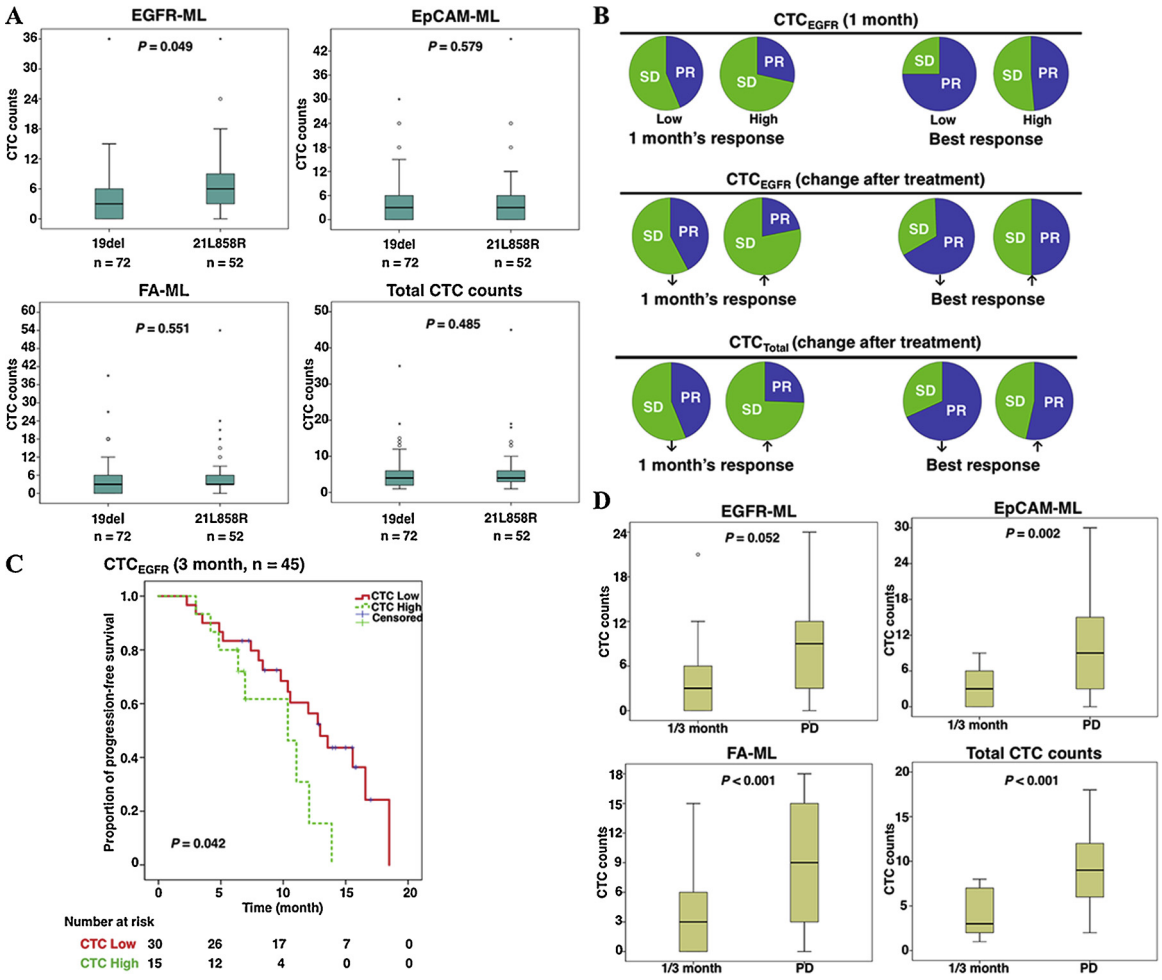

Fig. 4. Correlations between clinical information and CTC.

(A) Correlation between EGFR mutations and baseline CTC counts.

(B) Proportions of patients with PR or SD in the different CTC groups.

(C) Survival curves of PFS according to CTC_{EGFR} at 3 months after EGFR-TKI treatment.

(D) Comparison of CTC counts between PD and previous time points.

CTC_{EGFR}, CTC_{EpCAM}, CTC_{FA} and CTC_{Total} are used to represent CTC counts by different ML and total CTC numbers, respectively.

CI, confidence interval; CTC, circulating tumor cells; EGFR, epidermal growth factor receptor; EGFR-TKI, epidermal growth factor receptor tyrosine kinase inhibitors; EpCAM, epithelial cell adhesion molecule; FA, folic acid; PD, progressive disease; PR, partial response; SD, stable disease; 19del, EGFR exon 19 deletions; 21L858R, EGFR exon 21 leucine-to-arginine substitutions at position 858.

3.5. PFS and CTC counts

The characteristics of the 55 patients used for PFS analysis are shown in Table S6. In 34 patients (62%), PD occurred at the study cut-off date. The median PFS for 55 patients was 12.8 months (95% CI 10.6–15 months). The correlation between PFS and CTC counts is shown in Table S7. Patients with lower CTC_{EGFR} at 3 months after EGFR-TKI achieved a longer PFS than patients with higher CTC_{EGFR} [13 months (95% CI 10.6–15.3 months) vs. 10.4 months (95% CI 5.9–14.8 months), HR = 2.4, P = 0.042; Fig. 4C]. Multivariate survival analysis after adjusting for gender, CTC_{EGFR} at 3 months, clinical stage, and EGFR mutant sites also confirmed the above results [HR = 2.53 (95% CI 1.02–6.25), P = 0.046; Table S8]. No correlation was observed between PFS and CTC counts measured by other ML.

3.6. CTC change in PD patients

The characteristics of 22 patients used for PD analysis are shown in Table S9. Regardless of the ML type, the median CTC counts increased significantly at the onset of PD when compared to the counts at 3 months or 1 month (CTC_{EGFR}: 9 vs. 3, P = 0.052; CTC_{EpCAM}: 9 vs. 3, P = 0.002; CTC_{FA}: 9 vs. 3, P < 0.001; CTC_{Total}: 9 vs. 3, P < 0.001; Fig. 4D and Table S10). Although most patients at PD exhibited higher CTC counts (CTC_{EGFR}: 12/22, 55%; CTC_{EpCAM}: 15/22, 68%; CTC_{FA}: 17/22, 77%; CTC_{Total}: 18/22, 82%; Fig. 5A-D left panels; Table S11), the remaining showed unchanged or even decreased CTC counts (CTC_{EGFR}: 45%; CTC_{EpCAM}: 32%; CTC_{FA}: 23%; CTC_{Total}: 18%; Fig. 5A-D right panels; Table S11). The reasons for RECIST-PD of the 22 patients are outlined in Table S12. Thirteen patients (59%) were diagnosed with PD due to new metastatic lesions in the lung, bone, and brain, among which 9 patients (69%) of them had increased CTC_{EGFR} at RECIST-PD, while 8 (62%), 10 (77%), and 11 patients (85%) had high CTC_{EpCAM}, CTC_{FA}, and CTC_{Total}, respectively. In addition, after excluding 6 patients with lung lesions, 7 (100%), 5 (71%), 7 (100%), and 7 (100%) patients had increased CTC_{EGFR}, CTC_{EpCAM}, CTC_{FA}, and CTC_{Total}, respectively.

3.7. Case studies

Baseline information of the 3 representative cases are provided in Table S13.

CTC counts started to increase before RECIST-PD: For case #155, we observed that CTC_{EGFR} correlated with tumor size, as it decreased

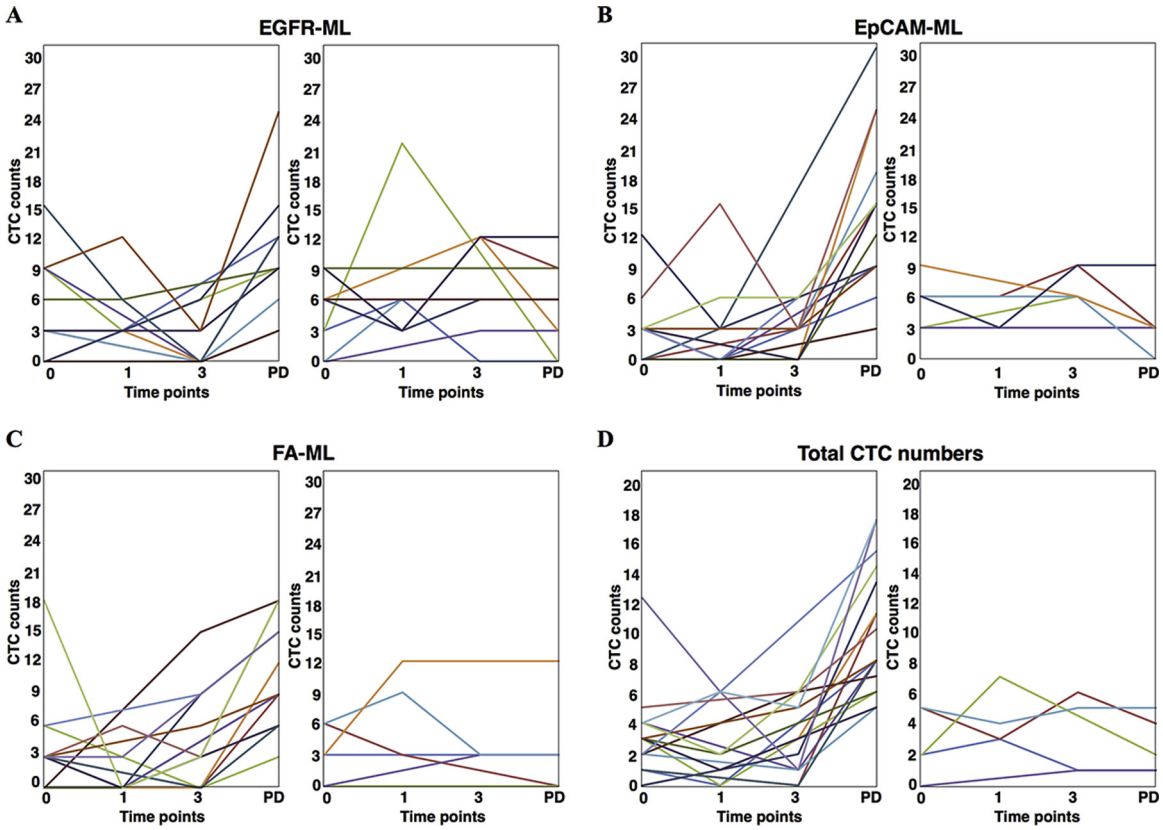

Fig. 5. Dynamic changing curves of CTC counts in the process of EGFR-TKI treatment for patients occurred PD.
(A) CTC numbers identified by EGFR-ML; (B) CTC numbers identified by EpCAM-ML; (C) CTC numbers identified by EpCAM-ML; (D) Total CTC numbers.
Each line represents the change of CTC number from an individual. For each ML, CTC counts of most patients increased (left panel of each bead) while CTC counts of other patients remained unchanged or even decreased (right panel of each bead).
CTC, circulating tumor cells; EGFR-TKI, epidermal growth factor receptor tyrosine kinase inhibitors; EpCAM, epithelial cell adhesion molecule; FA, folic acid; ML, magnetic liposome; PD, progressive disease.

with the diminishing tumor after icotinib treatment. The tumor size was the smallest after three months of treatment, at which point CTC_{EGFR} was undetectable. With the gradual enlargement of the metastatic lung lesion, the CTC_{EGFR} started to increase until PD occurred due to the progression of the primary lung lesion and new brain metastases at 10 months after treatment. The CTC_{Total} showed the same trend, whereas this trend was not observed for CTC_{EpCAM} and CTC_{FA} (Fig. 6A).

CTC counts continued to increase after RECIST-PD: Case #11 was treated with icotinib and achieved PR as the best response at 7 months after treatment, at this time, CTC_{EGFR} had decreased to zero. Due to the enlargement of lung lesions, RECIST-PD was determined after 13 months of treatment. We continued to administer icotinib up to 16 months when we observed no clinical benefit due to further progression of lung lesions and the emergence of new bone lesions (clinical-PD). The CTC_{EGFR} increased from 6 at RECIST-PD to 12 at clinical-PD. The CTC_{Total} also showed a similar trend, and the CTC_{FA} also increased after RECIST-PD but could not be detected prior to PD (Fig. 6B). Case #48 achieved SD as the best response, and CTC_{EGFR} was positively correlated with lung tumor size. PD occurred after 10 months of treatment, and gefitinib treatment was continued due to the gradual progression. The CTC_{EGFR}, however, continued to increase up to month 17, and clinical-PD was observed at month 21. CTC_{EpCAM} and CTC_{Total} also increased after RECIST-PD (Fig. 6C).

4. Discussion

In this study, we established a robust CTC enrichment method using EGFR immuno-magnetic beads. Using this detection system, we found that EGFR-activating NSCLC patients with a lower CTC_{EGFR} at 3 months after first-line EGFR-TKI treatment had a PFS that was 2.5 months longer compared to patients with a higher CTC_{EGFR}. In addition, patients with non-increased CTC_{EGFR} were more likely to achieve PR, and the CTC counts were significantly increased at RECIST-PD. To the best of our knowledge, this is the first study to evaluate the predictive value of CTC enumeration based on an EGFR immuno-magnetic beads capture method in first-line EGFR-TKI efficacy in patients with advanced NSCLC.

Non-invasive CTC, which are disseminated from primary tumor cells, have the potential to obviate the limitations that are associated with solid tumor tissues for monitoring cancer treatment [23]. Currently, mature CTC detection methods include immuno-magnetic liposomal fluorescence identification, CTC biopsy, and CanPatrol of the CellSearch system. The prognostic value of CTC enumeration has been studied in several types of metastatic cancer [17–19,24–26]. However, these studies mainly used the CellSearch system, which may fail to detect the CTC with downregulated EpCAM levels due to EMT. In addition, the predictive value of CTC enumeration in NSCLC regarding EGFR-TKI efficacy has not yet been studied. Therefore, we established a CTC enrichment system using liposomal EGFR immuno-magnetic beads, and assessed its performance in predicting first-line EGFR-TKI response in patients with advanced NSCLC compared to the EpCAM- and FA-based CTC enrichment system. Our study showed that the liposomal encasing had two significant advantages: 1) it prevented oxidation of the magnetic nanoparticles and optimized the magnetic separation, and 2) increased the concentration of antibodies that enhanced the CTC recovery rate.

The utility of CTC_{EGFR} in predicting EGFR-TKI efficacy was investigated using RECIST criteria. Patients with non-increased CTC_{EGFR}

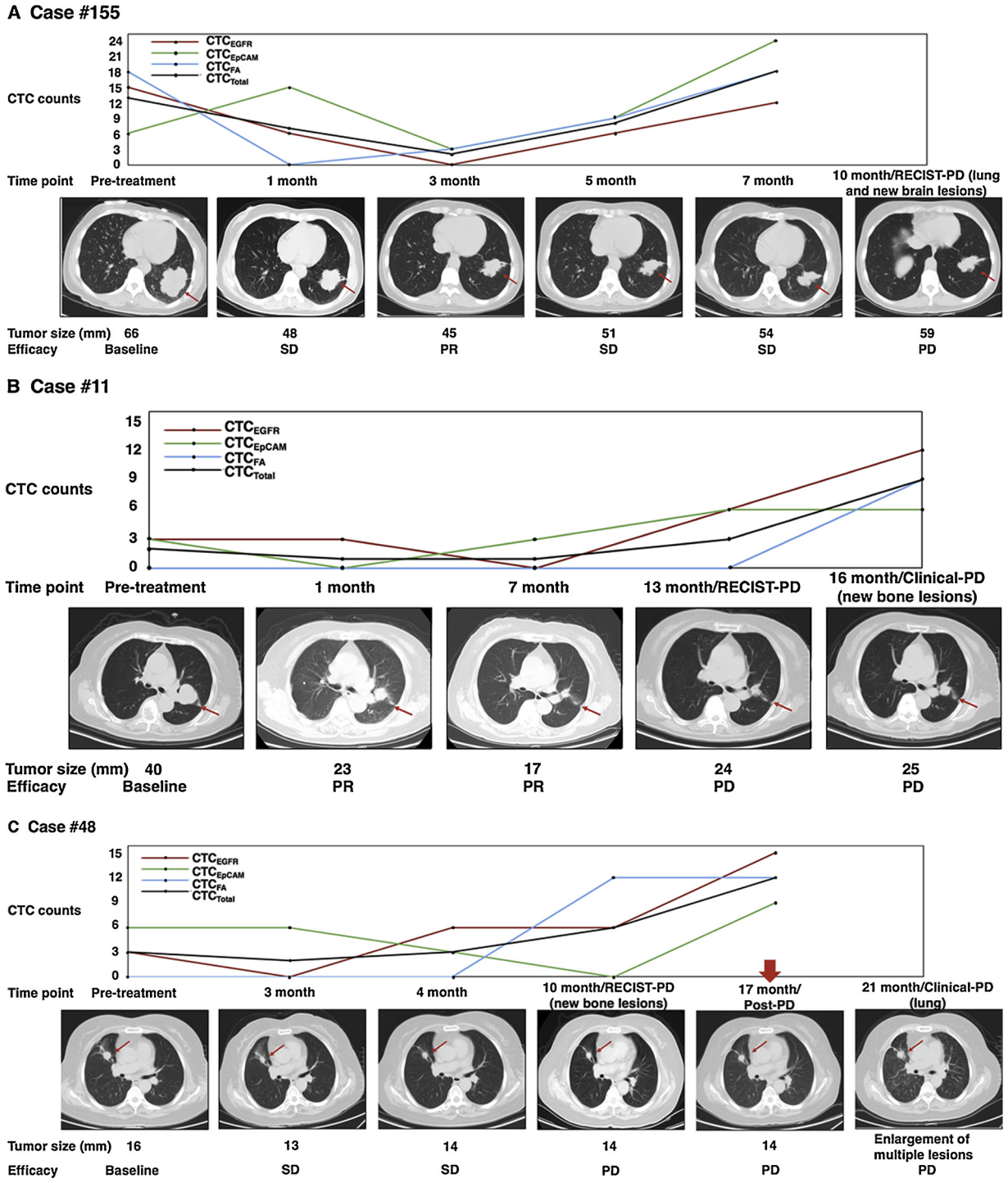

Fig. 6. Relationship between CTC number change and EGFR-TKI efficacy in representative cases.

After 3 months' EGFR-TKI treatment, lung lesion size gradually increased and CTC_{EGFR} increased up to RECIST-PD because of the enlargement of primary lung lesion and occurrence of new brain metastases lesions at 10 months (A); CTC_{EGFR} increased from 6 at RECIST-PD to 12 at clinical-PD (B); Seven months after RECIST-PD, CTC_{EGFR} continued to increase and clinical-PD was achieved after another 4 months (C).

CTC_{EGFR}, CTC_{EpCAM}, CTC_{FA}, CTC_{Total} are used to represent CTC counts by different ML and total CTC numbers, respectively.

CTC, circulating tumor cells; EpCAM, epithelial cell adhesion molecule; EGFR-TKI, epidermal growth factor receptor tyrosine kinase inhibitors; FA, folic acid; PD, progressive disease.

were more likely to achieve PR after 1 month of EGFR-TKI treatment when compared to patients with increased CTC_{EGFR}. These findings indicated that a decreased or unchanged CTC count after EGFR-TKI treatment may predict a better response. In addition, patients with lower CTC_{EGFR} at 3 months after first-line EGFR-TKI treatment may achieve a PFS that is increased with more than 2 months compared to those with a higher CTC_{EGFR}. Several studies have shown that continuous use of EGFR-TKIs beyond RECIST-PD may render patients to acquire additional survival benefits from targeted drugs [27,28]. This indicated that a RECIST-defined PD can be used to decide chemotherapy discontinuation. However, it may not be a suitable standard for targeted therapies. In this study, CTC counts measured by all three

ML increased at RECIST-PD, thereby suggesting the potential predictive value of CTC changes in EGFR-TKI response at the PD time point. Interestingly, we noticed that in some cases, CTC_{EGFR} increased prior to RECIST-PD, and continued to increase up to discontinuation of the drug. These findings were significant since in some patients an increased CTC_{EGFR} may appear earlier than the RECIST-defined PD. However, whether CTC_{EGFR} can be used as an indicator for EGFR-TKI discontinuation needs to be evaluated in future studies.

In addition to counting CTC numbers, the EGFR immuno-magnetic beads we designed have the potential to detect EGFR mutations in blood (data not shown). Our preliminary data showed that the initial mutation cannot be detected in two of the 3 PD samples.

Our study has some limitations. First, since this was a single-center study with a relatively small sample size, our findings should be interpreted with caution. Second, due to the study design and relatively shorter follow-up time, the overall survival could not be analyzed. Therefore, the independent predictive value of CTC enumeration in the survival of EGFR-TKI receiving patients could not be assessed. In addition, it is important to test whether some of the CTC captured by EGFR-ML cannot be captured by EpCAM-ML because of the EMT process in the future.

Taken together, our findings showed that it is feasible to establish a CTC enrichment system using antibody modified EGFR-ML. In addition, CTC enumeration by EGFR-ML has the potential to predict the response of NSCLC patients to first-line EGFR-TKI and may supplement RECIST in dynamically monitoring of patients.

Author contributions

Liyan Jiang, Shaohua Cui, Zonghai Li and Xiaofei Liang conceived the study. Liyan Jiang, Shaohua Cui and Xiaofei Liang coordinated the study. Liwen Xiong, Liyan Jiang and Yizhuo Zhao selected and contributed clinical samples. Xiaofei Liang performed CTC detection using three immunomagetic beads from peripheral blood samples and arranged CTC enumeration data. Yiqian Ni, Shaohua Cui and Yizhuo Zhao collected clinical data and assessed patients' response to EGFR-TKI. Shaohua Cui incorporated CTC enumeration data with clinical data and did comprehensive statistical analyses. Shaohua Cui and Xiaofei Liang prepared the manuscript. All authors read, commented on the manuscript. All authors confirmed and approved the final version for submission.

Funding

This project was supported by the Medical Guidance Projects of Shanghai Science and Technology Committee (Grant No. 15411961500, 17411971100).

Conflicts of interest

All authors have no conflicts of interest to declare.

Acknowledgements

The authors would like to thank Xiaojie Tao for blood sample collection at Shanghai Chest Hospital, Shanghai Jiao Tong University.

Appendix A. Supplementary data

Supplementary material related to this article can be found, in the online version, at doi:https://doi.org/10.1016/j.lungcan.2019.04.003.

References

[1] M.G. Kris, B.E. Johnson, L.D. Berry, D.J. Kwiatkowski, A.J. Iafrate, I.I. Wistuba, et al., Using multiplexed assays of oncogenic drivers in lung cancers to select targeted drugs, JAMA 311 (2014) 1998–2006.
[2] Y. Shi, J.S. Au, S. Thongprasert, S. Srinivasan, C.M. Tsai, M.T. Khoa, et al., A prospective, molecular epidemiology study of EGFR mutations in Asian patients with advanced non-small-cell lung cancer of adenocarcinoma histology (PIONEER), J. Thorac. Oncol. 9 (2014) 154–162.
[3] T.J. Lynch, D.W. Bell, R. Sordella, S. Gurubhagavatula, R.A. Okimoto, B.W. Brannigan, et al., Activating mutations in the epidermal growth factor receptor underlying responsiveness of non-small-cell lung cancer to gefitinib, New England J. Med. Surg. Collat. Branches Sci. 350 (2004) 2129–2139.
[4] J.G. Paez, P.A. Jänne, J.C. Lee, S. Tracy, H. Greulich, S. Gabriel, et al., EGFR mutations in lung cancer: correlation with clinical response to gefitinib therapy, Science 304 (2004) 1497–1500.
[5] National Comprehensive Cancer Network, (NCCN) Clinical Practice Guidelines in Oncology. Non-Small Cell Lung Cancer, Version 4, (2018) Accessed April 26, 2018 https://www.nccn.org/professionals/physician_gls/pdf/nscl.pdf.
[6] M. Yanagita, A.J. Redig, C.P. Paweletz, S.E. Dahlberg, A. O'Connell, N. Feeney, et al., A prospective evaluation of circulating tumor cells and cell-free DNA in EGFR-Mutant non-small cell lung Cancer patients treated with erlotinib on a phase II trial, Clin. Cancer Res. 22 (2016) 6010–6020.
[7] M. Murtaza, S.J. Dawson, D.W. Tsui, D. Gale, T. Forshew, A.M. Piskorz, et al., Non-invasive analysis of acquired resistance to cancer therapy by sequencing of plasma DNA, Nature 497 (2013) 108–112.
[8] K. Ross, E. Pailler, V. Faugeroux, M. Taylor, M. Oulhen, N. Auger, et al., The potential diagnostic power of circulating tumor cell analysis for non-small-cell lung cancer, Expert Rev. Mol. Diagn. 15 (2015) 1605–1629.
[9] E.I. Galanzha, E.V. Shashkov, T. Kelly, J.W. Kim, L. Yang, V.P. Zharov, In vivo magnetic enrichment and multiplex photoacoustic detection of circulating tumour cells, Nat. Nanotechnol. 4 (2009) 855–860.
[10] A.A. Ghazani, C.M. Castro, R. Gorbatov, H. Lee, R. Weissleder, Sensitive and direct detection of circulating tumor cells by multimarker μ-nuclear magnetic resonance, Neoplasia 14 (2012) 388–395.
[11] W. Onstenk, W. de Klaver, R. de Wit, M. Lolkema, J. Foekens, S. Sleijfer, The use of circulating tumor cells in guiding treatment decisions for patients with metastatic castration-resistant prostate cancer, Cancer Treat. Rev. 46 (2016) 42–50.
[12] J.G. Lohr, V.A. Adalsteinsson, K. Cibulskis, A.D. Choudhury, M. Rosenberg, P. Cruz-Gordillo, et al., Whole-exome sequencing of circulating tumor cells provides a window into metastatic prostate cancer, Nat Biotech 32 (2014) 479–484.
[13] M.G. Krebs, A.G. Renehan, A. Backen, S. Gollins, I. Chau, J. Hasan, et al., Circulating tumor cell enumeration in a phase II trial of a four-drug regimen in advanced colorectal Cancer, Clin. Colorectal Cancer 14 (115-22) (2015) e1–2.
[14] G. Heller, R. McCormack, T. Kheoh, A. Molina, M.R. Smith, R. Dreicer, et al., Circulating tumor cell number as a response measure of prolonged survival for metastatic castration-resistant prostate Cancer: a comparison with prostate-specific antigen across five randomized phase III clinical trials, J. Clin. Oncol. 36 (2018) 572–580.
[15] J.M. Hou, M.G. Krebs, L. Lancashire, R. Sloane, A. Backen, R.K. Swain, et al., Clinical significance and molecular characteristics of circulating tumor cells and circulating tumor microemboli in patients with small-cell lung cancer, J. Clin. Oncol. 30 (2012) 525–532.
[16] E.A. Punnoose, S. Atwal, W. Liu, R. Raja, B.M. Fine, B.G. Hughes, et al., Evaluation of circulating tumor cells and circulating tumor DNA in non-small cell lung cancer: association with clinical endpoints in a phase II clinical trial of pertuzumab and erlotinib, Clin. Cancer Res. 18 (2012) 2391–2401.
[17] M. Cristofanilli, G.T. Budd, M.J. Ellis, A. Stopeck, J. Matera, M.C. Miller, et al., Circulating tumor cells, disease progression, and survival in metastatic breast cancer, N. Engl. J. Med. 351 (2004) 781–791.
[18] S.J. Cohen, C.J. Punt, N. Iannotti, B.H. Saidman, K.D. Sabbath, N.Y. Gabrail, et al., Relationship of circulating tumor cells to tumor response, progression-free survival, and overall survival in patients with metastatic colorectal cancer, J. Clin. Oncol. 26 (2008) 3213–3221.
[19] J.S. de Bono, H.I. Scher, R.B. Montgomery, C. Parker, M.C. Miller, H. Tissing, et al., Circulating tumor cells predict survival benefit from treatment in metastatic castration-resistant prostate cancer, Clin. Cancer Res. 14 (2008) 6302–6309.
[20] X. Liang, H. Wang, X. Jiang, J. Chang, Development of monodispersed and functional magnetic polymeric liposomes via simple liposome method, J. Nanopart. Res. 12 (2010) 1723–1732.
[21] J. Ding, K. Wang, W.J. Tang, D. Li, Y.Z. Wei, Y. Lu, et al., Construction of epidermal growth factor receptor peptide magnetic nanovesicles with lipid bilayers for enhanced capture of liver Cancer Circulating tumor cells, Anal. Chem. 88 (2016) 8997–9003.
[22] Y. Cao, X. Liang, L. Li, R. Pan, K. Wang, C. Xiao, et al., High-efficiency EpCAM/EGFR-PLGA immunomagnetic beads with specific recognition on circulating tumor cells in colorectal Cancer, J. Biomed. Nanotechnol. 13 (2017) 758–766.
[23] E.S. Lianidou, A. Strati, A. Markou, Circulating tumor cells as promising novel biomarkers in solid cancers, Crit. Rev. Clin. Lab. Sci. 51 (2014) 160–171.
[24] S.J. Cohen, C.J. Punt, N. Iannotti, B.H. Saidman, K.D. Sabbath, N.Y. Gabrail, et al., Prognostic significance of circulating tumor cells in patients with metastatic colorectal cancer, Ann. Oncol. 20 (2009) 1223–1229.
[25] D.C. Danila, G. Heller, G.A. Gignac, R. Gonzalez-Espinoza, A. Anand, E. Tanaka, et al., Circulating tumor cell number and prognosis in progressive castration-resistant prostate cancer, Clin. Cancer Res. 13 (2007) 7053–7058.
[26] S. Mocellin, D. Hoon, A. Ambrosi, D. Nitti, C.R. Rossi, The prognostic value of circulating tumor cells in patients with melanoma: a systematic review and meta-analysis, Clin. Cancer Res. 12 (2006) 4605–4613.
[27] K. Park, Kim S.W. Yu CJ, M.C. Lin, V. Sriuranpong, C.M. Tsai, et al., First-line erlotinib therapy until and beyond response evaluation criteria in solid tumors progression in asian patients with epidermal growth factor receptor mutation-positive non-small-Cell lung Cancer: the ASPIRATION study, JAMA Oncol. 2 (2016) 305–312.
[28] K. Nishie, T. Kawaguchi, A. Tamiya, T. Mimori, N. Takeuchi, Y. Matsuda, et al., Epidermal growth factor receptor tyrosine kinase inhibitors beyond progressive disease: a retrospective analysis for Japanese patients with activating EGFR mutations, J. Thorac. Oncol. 7 (2012) 1722–1727.